

Quantitative Characterization of Impacts of Coupled Geomechanics and Flow on Safe and Permanent Geological Storage of CO₂ in Fractured Aquifers

DE-FE0023305

Philip H. Winterfeld
Colorado School of Mines

U.S. Department of Energy

National Energy Technology Laboratory

Mastering the Subsurface Through Technology, Innovation and Collaboration:

Carbon Storage and Oil and Natural Gas Technologies Review Meeting

August 16-18, 2016

Presentation Outline

- Benefit to the Program
- Project Overview: Goals and Objectives
- Technical Status
- Accomplishments to Date
- Summary
- Appendix

Benefit to the Program

- Laboratory studies of rock deformation, fracturing with coupled geomechanical modeling to quantify effects of geomechanics and flow on safe and permanent geological storage of CO₂
- Understanding of geomechanical effects on CO₂ flow and storage in fractured reservoirs; develop modeling tools for assessment of CO₂ geo-storage systems
- Technology developed in project will contribute to our ability to predict CO₂ storage capacity in geologic formations to within ± 30 percent

Project Overview: Goals and Objectives

- Understanding and correlations for injection pressure induced geomechanical effects (rock deformation, fracturing) on CO₂ storage systems, through lab experiments
- Incorporate above into simulators (TOUGH2-CSM and TOUGH-FLAC) to model CO₂ injection induced rock mechanical processes associated with CO₂ storage in reservoirs
- Quantify flow, storage, and potential leakage pathways; develop remediation measures when needed

Technical Status

2) Laboratory studies of effects of geomechanics on CO₂ flow and transport properties in fractured rock

Rock Property Tests

- Three different rock types: concrete, sandstone and shale
- Acoustic test - compressional and shear wave velocities, bulk modulus, Poisson's ratio
- Permeability and porosity - CMS-300 (CoreLab), helium flow through sample under confining stress
- Brazilian test - splitting tensile strength test
- Uniaxial compression test - compressional strength, no confining stress, sample load increases until failure
- Specific heat - calorimeter, scale, thermocouple - energy balance yields heat capacity

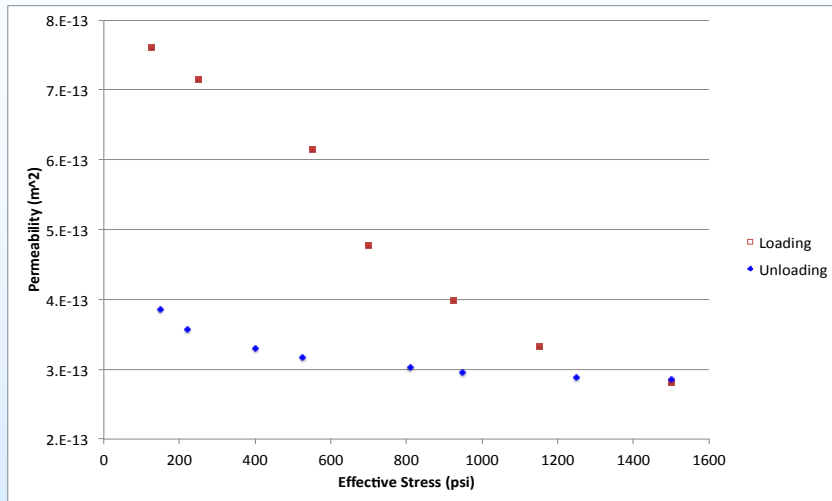
Rock Property Results

	Concrete	Sandstone	Shale
Sample Origin	Type II Portland Cement	Williams Fork Outcrop, West CO	Niobrara Formation Boulder, CO
Young's Mod, GPa, Poisson's Ratio	30.0; 0.243	118.3; 0.142	49.3; 0.268
Porosity, %; Perm, mD	9.56; 0.009	11.47; 0.349	6.65; 0.001
Tensile Str., MPa (Brazilian test)	2.878	4.505	8.455
Uniaxial Compres. Str., MPa	37.343	41.457	54.585
Sp. Heat, J/kg·K	891	857	990

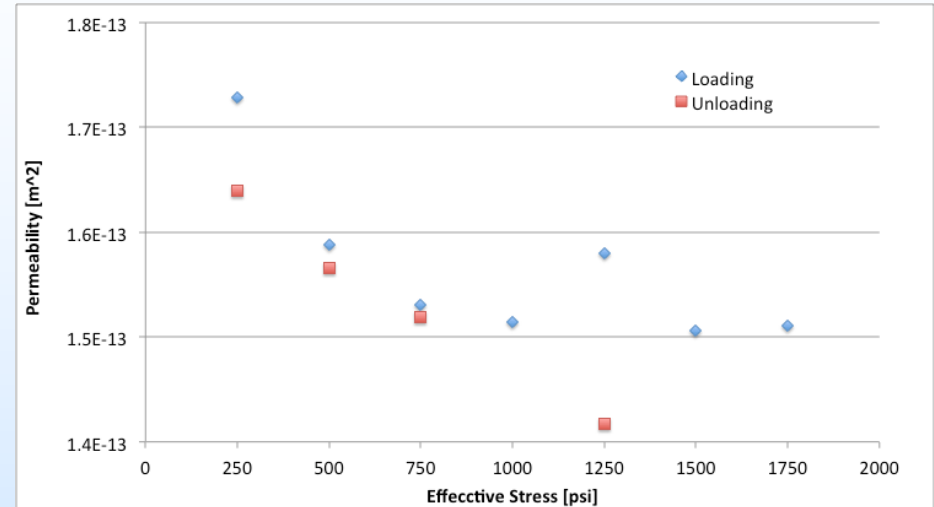
Permeability vs Effective Stress

- Fracture sample (Brazilian test), place spacers at corners
- Gray Berea fractures well; other samples showed splaying
- Reassemble core, wrap core in sleeves, place in core holder
- Confining pressure applied, fluid flows through sample at specific rates, measure differential pressure
- Compute permeability versus effective stress
- CT scan core at each flow rate – change in fracture aperture

Gray Berea Permeability



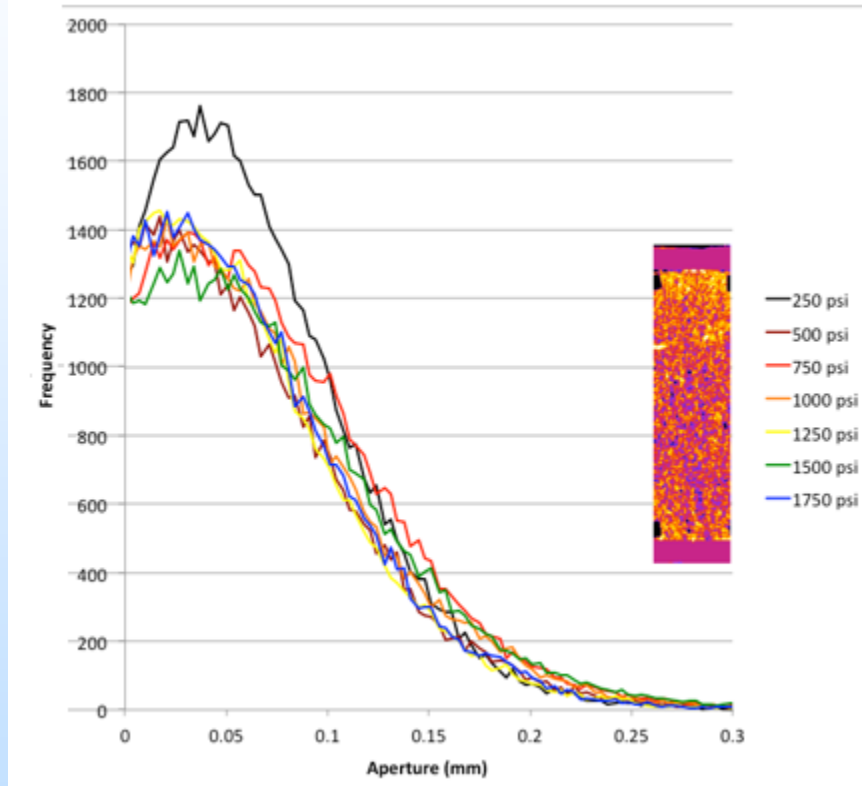
Air



Brine

- Air permeability 2X brine permeability
- Brine may mobilize cuttings from the coring
- Gas flow rate not large enough for such mobilization

Gray Berea Aperture



- Little change in distribution beyond 500 psi
- Inset is image of aperture map at 250 psi
- Aperture highest at ends and in vicinity of spacers (black regions in figure)

Future Work

- Measurements of permeability versus effective stress for scCO₂ are underway and will be continued
- scCO₂ equipment is similar to that for brine experiments; temperature control added to keep CO₂ in supercritical region
- Additional measurements of permeability versus effective stress for brine will be carried out

3) Laboratory studies of CO₂ and brine injection induced fracturing

Equipment

- Tri-axial loading system: three pistons - two horizontal, one vertical; provide up to 4.5K psi horizontal, 6.0K psi vertical stress on 8 inch cube
- Injection pump - Teledyne ISCO 500HPx; 10 to 5000 psi - ideal for brine and super-critical CO₂; 507.4 ml capacity before refilling
- Data acquisition devices - Type T thermocouples, (-200 to 350 °C); pressure transducers - up to 3000 psi



Initial Experiments

- Better understand fracturing process, establish test procedure
- Concrete – 8 inch cubic block, 6 inch borehole from top
- Confining stress: 500, 750, 1000 psi in x-, y-, z-directions
- Low pressure samples fracturing around 450 psi
- High pressure samples fracturing around 1000 psi

Low Pressure Sample

- Flow rate increased from 5 to 50 ml/min
- Fracture initiation at 1600 sec, 450 psi
- Second peak – flow rate 200 ml/min, opened fracture

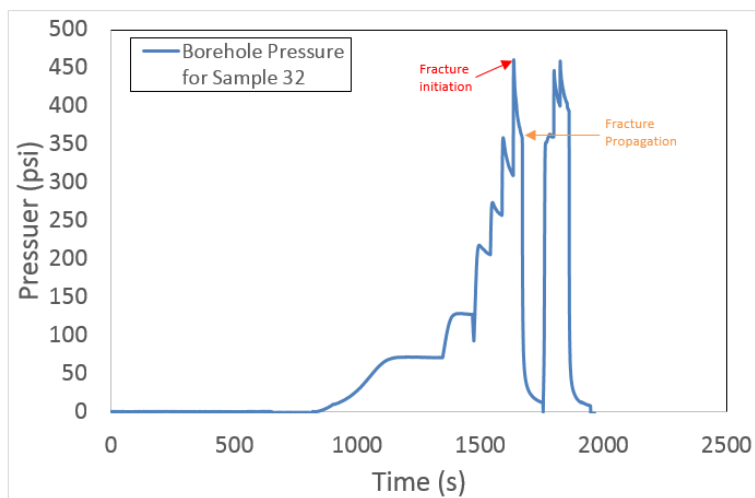


Figure 3.4: Borehole Pressure Profile of Sample #32.

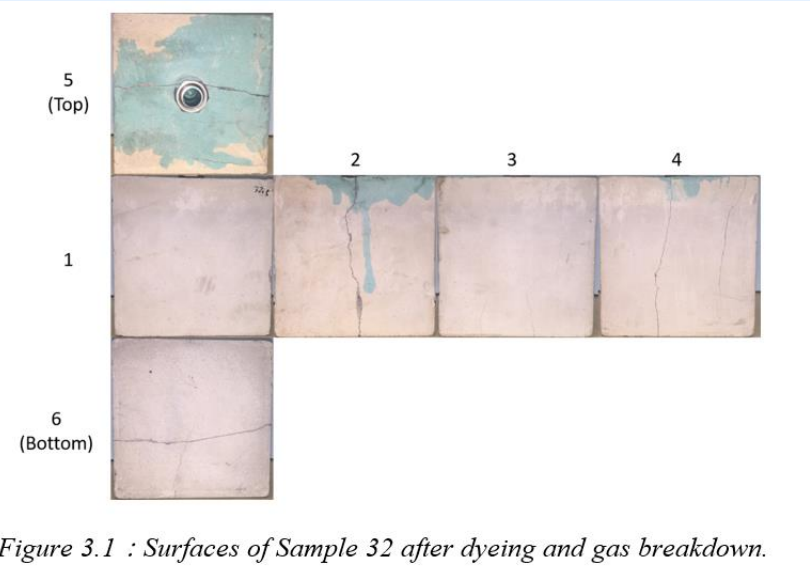


Figure 3.1 : Surfaces of Sample 32 after dyeing and gas breakdown.

High Pressure Sample

- Wellbore filled with brine
- Fracture initiation at 500 sec, 1100 psi
- Flow rate increased to verify fractures; no fractures on surface

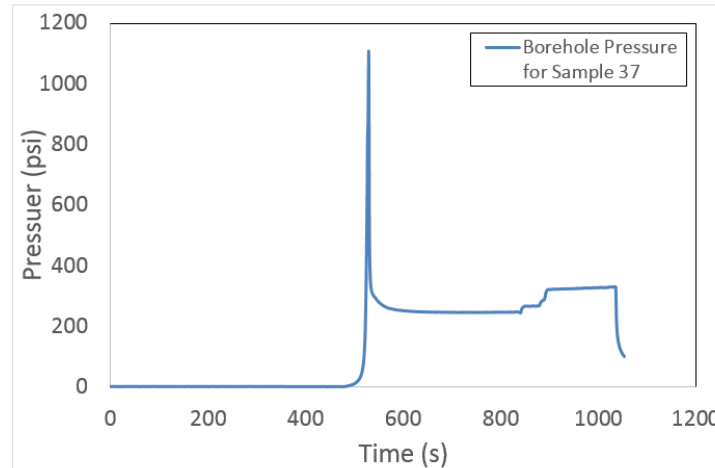


Figure 3.7: Borehole Pressure Profile of Sample 37.

Later Experiment

- Constant flow rate, 40ml/min
- x-, y-, z- confining stresses: 1000, 1500, 2000 psi
- Pressure peaks at 2424 psi
- Major fracture plane across the bore hole; generally perpendicular to minimum stress direction



scCO₂ Experiment

- Same equipment as brine fracturing plus temperature control
- Field conditions above CO₂ critical point (31 °C, 7.38 MPa), so concrete samples preheated before experiment
- Confining stress: 1000, 1500, 2000 psi in x-, y-, z- directions, injection rate 40ml/min
- Fractured at 1145 psi (43 minutes), pump refilled at 24 min
- Fracture visualized by injecting dye solution and breaking down with nitrogen; straight fracture with smooth surfaces

scCO₂ Experiment, II

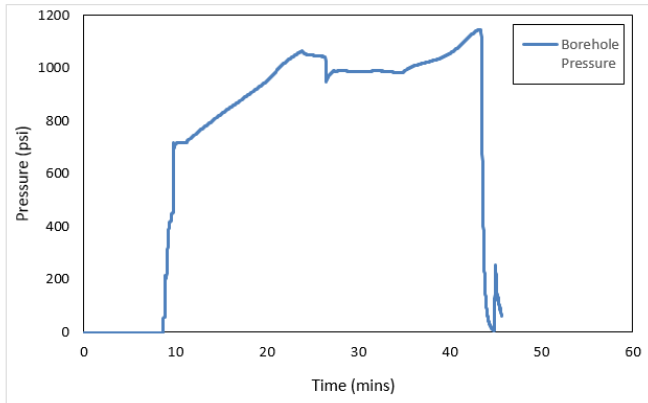


Figure 3.28: Borehole pressure during CO₂ injection.



Figure 3.33: Fracture planes of Sample 27 after dyeing and gas breakdown.

Future Work

- Additional experiments using scCO₂
- Experimental studies of fracture propagation to be done beginning of third year

4) Development of CO₂ flow and geomechanics-coupled models for modeling fracturing growth

TOUGH2-CSM

Mean Stress Equation

- Hooke's law for a thermo-multi-poroelastic medium + stress equilibrium equation + strain tensor definition = Navier equation, then take divergence

$$\nabla \cdot \left[\frac{3(1-\nu)}{1+\nu} \nabla \tau_m + \mathbf{F}_b - \frac{2(1-2\nu)}{1+\nu} \nabla \left(\sum_j (\alpha_j P_j + 3\beta K \omega_j T_j) \right) \right] = 0$$

- Trace of Hooke's law: volumetric strain equation

$$K \varepsilon_v = \tau_m - \sum_j (\alpha_j P_j + 3\beta K \omega_j (T_j - T_{ref}))$$

Stress Tensor Components

- Derivatives of thermo-multi-poroelastic Navier equation vector components are zero:

- Normal stresses:

$$\frac{\partial^2}{\partial x^2} [h(\mathbf{P}, \mathbf{T})] + \frac{3}{2(1+\nu)} \frac{\partial^2}{\partial x^2} [\tau_m - h(\mathbf{P}, \mathbf{T})] + \frac{1}{2} \nabla^2 \left[\tau_{xx} - h(\mathbf{P}, \mathbf{T}) - \frac{3\nu}{1+\nu} (\tau_m - h(\mathbf{P}, \mathbf{T})) \right] + \frac{\partial F_{b,x}}{\partial x} = 0$$

- Shear stresses:

$$\frac{\partial^2}{\partial x \partial y} [h(\mathbf{P}, \mathbf{T})] + \frac{3}{2(1+\nu)} \frac{\partial^2}{\partial x \partial y} [\tau_m - h(\mathbf{P}, \mathbf{T})] + \frac{1}{2} \nabla^2 \tau_{xy} + \frac{1}{2} \left(\frac{\partial F_{b,y}}{\partial x} + \frac{\partial F_{b,x}}{\partial y} \right) = 0$$

Stress Tensor Solution

- Mean stress variables (P, X, T, T_m) solved for first
- Stress tensor components then calculated
- Stress tensor components depend only on mean stress variables; 1x1 Jacobian; fast calculation
- Formulation verified using analytical solutions – displacement of semi-infinite medium and Mandel-Cryer effect

Stress Tensor Initialization

- No shear stresses, z-direction dependence only

- zz-component from equilibrium equation:

$$\frac{\partial \tau_{zz}}{\partial z} + F_{b,z} = 0$$

- xx- and yy-stresses from geomechanical formulation

$$\frac{\partial^2}{\partial z^2} \left[\tau_{xx} - h(P, T) - \frac{3\nu(\tau_m - h(P, T))}{1 + \nu} \right] = 0$$

- Reference stress, stress ratios at reference elevation

$$\lim_{z \rightarrow z_0} \frac{\tau_{xx} - \tau_{xx,0}}{\tau_{zz} - \tau_{zz,0}} = R_{xz}$$

Stress Tensor Example

- Uniform grid
- Injection source at center
- Constant rock properties
- Constant injection rate
- Single phase
- Constant stress on boundaries

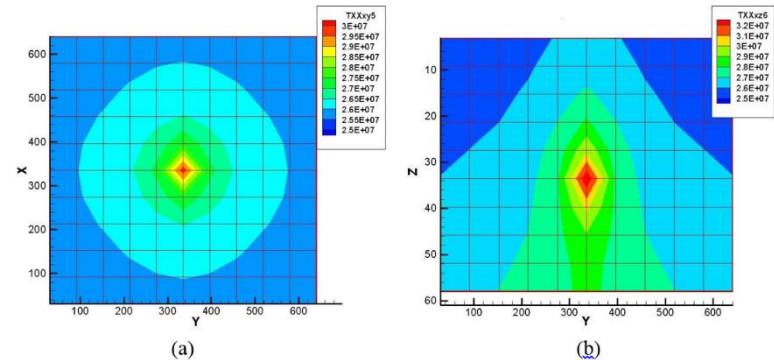


Figure 4.2.5. Normal xx -stress cross sections for xy -plane, $K=5$ (a) and xz -plane, $J=6$ (b) after three years of injection.

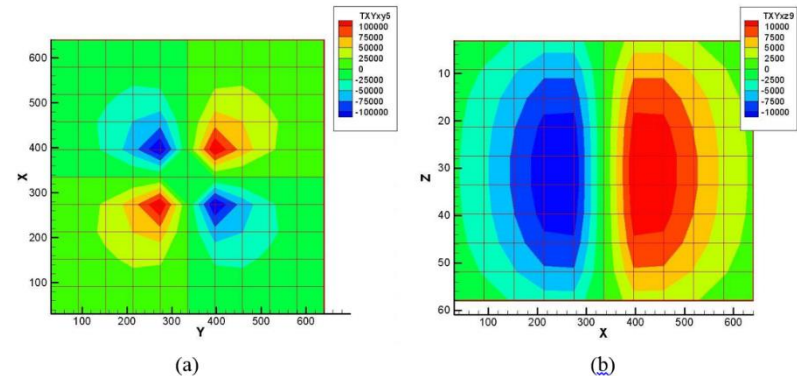


Figure 4.2.6. Shear xy -stress cross sections for xy -plane, $K=5$ (a) and xz -plane, $J=9$ (b) after three years of injection.

Rock Failure Modes

- Mohr-Coulomb failure – shear failure of fault

$$\tau > \mu\sigma' + C_0$$

- Mohr-Coulomb failure – shear failure of randomly fractured caprock

$$\sigma_1' > 3\sigma_3'$$

- Hydraulic fracturing due to pore pressure greater than minimum principal stress

$$P > \sigma_{\min} + \sigma_{tens}$$

Post Rock Failure

- Permeability and porosity correlated to stress for faults
- Fractured media – fracture aperture correlated to permeability:

$$k_f = \frac{b_f^2}{12\mu} \quad b_f = b_f(\tau') \quad \phi_f = \phi_f(\tau')$$

- Fracture growth and extension:

$$K_I > K_{IC} \quad d \approx \left(\frac{K_I - K_{IC}}{K_{IC}} \right)^n$$

TOUGH2-FLAC

Fracture Initiation and Growth

- Strain softening tensile behavior and softening of modulus
- Brittle to more ductile fracture behavior can be simulated by changing the strain softening characteristics
- Aperture changes with fracture propagation are related to the tensile strain normal to the fracture plane
- Permeability - cubic relation between fracture transmissivity and fracture aperture.

Model Verification

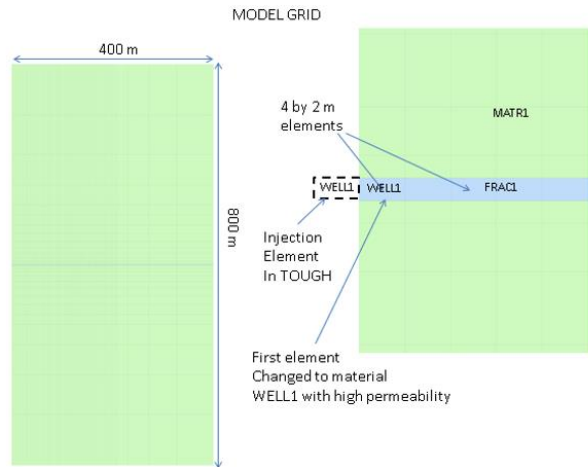


Figure 4.6. Model grid used for verification of TOUGH-FLAC fracture propagation model.

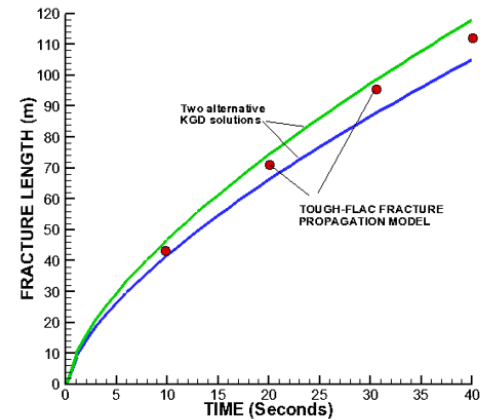


Figure 4.7. Comparison of TOUGH-FLAC fracture propagation results with that of the KGD model.

- Simulation test against solutions based on the KGD model
- 400 by 800 m grid, elements for fracture propagation
- Water injection at a constant rate

Future Work

- Incorporation of CO₂ injection-enhanced property and fracture correlations/models into reservoir simulators (Task 5)
- Concept and flow-mechanics coupled model validation using field data of stress and rock deformation measurement (Task 6)
- Development of modeling tools for identification of potential leakage risks (Task 7)

Accomplishments to Date, I

- Set up laboratory apparatuses for measuring rock properties
- Performed five rock property measurements on cores made from concrete, sandstone and shale
- Began measuring permeability versus effective stress (fractured gray Berea)
- Set up laboratory apparatuses for brine and CO₂ induced fracturing
- Performed fracturing experiments on concrete samples under various conditions, began scCO₂ ones

Accomplishments to Date, II

- Extended TOUGH2-CSM code to calculate stress tensor components
- Formulated rock failure simulation scenarios for TOUGH2-CSM
- Modified TOUGH2-FLAC to simulate fracture initiation and growth

Synergy Opportunities

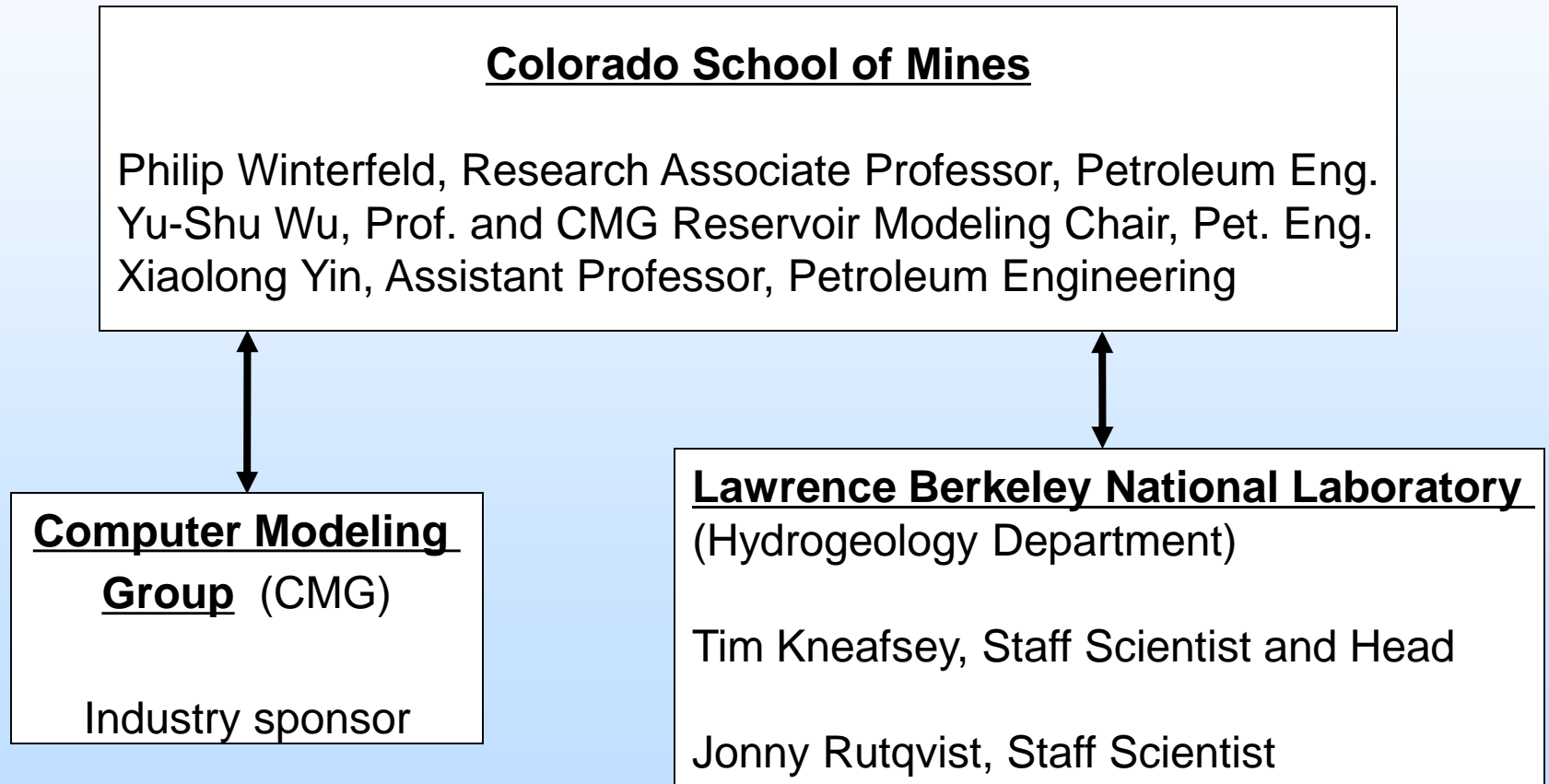
- Laboratory studies of rock deformation and fracturing
- Develop coupled geomechanical models for rock deformation and fracturing
- Rock property data obtained elsewhere can enhance our research efforts; rock property data obtained here could enhance other research efforts
- Our geomechanical models could be applied to other research efforts; other geomechanical models could suggest enhancements of ours

Summary

- We have established the procedures for the experimental portion of our project, began to obtain results, and have made the necessary modifications to our simulators with regard to them.
- We plan on completing most of the remaining tasks during the next period.

Appendix

Organization Chart



Gantt Chart

	Year 1				Year 2				Year 3			
Quarter	1	2	3	4	1	2	3	4	1	2	3	4
Task 1: Management and Planning												
Task 1: Management and Planning	■				■				■			
Task 2: Development of correlations of CO ₂ injection induced rock property variation by experiments												
Task 2.1: Obtaining rock cores and rock preparation	■											
Task 2.2: Permeability versus effective stress					■		■					
Task 2.3: scCO ₂ fracture permeability versus stress									■		■	
Task 3: Development of understanding and correlations of CO ₂ injection inducing fractures by experiments												
Task 3.1: Fracture initiation using brine	■											
Task 3.2: Fracture initiation using CO ₂					■		■					
Task 3.3: Fracture propagation									■			
Task 4: Development of CO ₂ flow and geomechanics -coupled models for modeling fracturing growth												
Task 4.1: Constitutive correlations for fracture initiation	■											
Task 4.2: Calculate stress tensor components			■									
Task 4.3: Simulate fracture initiation and growth (TOUGH2-CSM)					■		■					
Task 4.4: Simulate fracture initiation and growth (TOUGH2-FLAC)					■		■					
Task 4.5: Verification of TOUGH2-CSM and TOUGH-FLAC for fracturing modeling									■		■	

Gantt Chart, continued

Task 5: Incorporation of CO ₂ injection enhanced property and fracturing correlations/models into reservoir simulators												
Task 5.1: TOUGH2-CSM stress-dependent fracture permeability	█											
Task 5.2: TOUGH2-FLAC stress-dependent fracture permeability	█											
Task 5.3 Verification of TOUGH2-CSM and TOUGH-FLAC injection-induced property changes					█	█	█	█	█	█		
Task 6: Concept and flow-mechanics coupled model validation using field data of stress and rock deformation measurement												
Task 6.1: Validation of model for stress induced permeability changes in single fracture								█	█			
Task 6.2: Validation of model for fluid driven fracture propagation								█	█			
Task 6.3: Validation against deep fracture zone opening and surface uplift at In Salah									█	█	█	█
Task 6.4: Application of models to a generic large-scale sequestration site									█	█	█	█
Task 7: Development and application of advanced modeling and optimization schemes and integration												
Task 7.1: Inverse modeling model and optimization scheme										█	█	█
Task 7.2: Validation of the coupled model:										█	█	█

Bibliography

- Winterfeld, P. H. and Wu Y.-S., 2015, Simulation of Coupled Thermal-Hydrological-Mechanical Phenomena in Porous and Fractured Media, SPE 173210, presented at the SPE Reservoir Simulation Symposium, Houston, Texas, February 23-25, 2015
- Winterfeld, P. H. and Wu Y.-S., 2015 A Coupled Flow and Geomechanics Simulator for CO2 Storage in Fractured Reservoirs, to be presented at the TOUGH Symposium 2015, Lawrence Berkeley National Laboratory, Berkeley, CA, September 28-30, 2015
- Winterfeld, P. H. and Wu Y.-S., 2015, Simulation of Coupled Thermal-Hydrological-Mechanical Phenomena in Porous Media, SPE Journal, December 2016, p. 1041-1049.
- P. H. Winterfeld and Yu-S. Wu, Coupled Reservoir-Geomechanical Simulation of Caprock Failure and Fault Reactivation during CO2 Sequestration in Deep Saline Aquifers, to be presented at SPE Reservoir Simulation Conference, 20-22 February, 2017 in Montgomery, TX.